

Reduced order modeling and analysis of the human complement system

Adithya Sagar, Wei Dai[#], Mason Minot[#], and Jeffrey D. Varner*

School of Chemical and Biomolecular Engineering

Cornell University, Ithaca NY 14853

Running Title: A reduced order model of complement

To be submitted: *PLoS ONE*

Denotes equal contribution

*Corresponding author:

Jeffrey D. Varner,

Professor, School of Chemical and Biomolecular Engineering,

244 Olin Hall, Cornell University, Ithaca NY, 14853

Email: jdv27@cornell.edu

Phone: (607) 255 - 4258

Fax: (607) 255 - 9166

Abstract

Complement is an important pathway of innate immunity which plays a significant role in inflammation, and many disease processes. However, despite its importance, there has been a paucity of validated mathematical models of complement activation. In this study, we developed an ensemble of experimentally validated reduced order complement models. The modeling approach combined ordinary differential equations with logical rules to produce a complement model with a limited number of equations and parameters. The reduced order model, which described the lectin and alternative pathways, consisted of 18 differential equations with 28 parameters. Thus, the model was an order of magnitude smaller and included more pathways than comparable models in the literature. We estimated an ensemble of model parameters from *in vitro* time series measurements of the C3a and C5a complement proteins. Subsequently, we validated the model on unseen C3a and C5a measurements that were not used for model training. Despite its small size, the model was surprisingly predictive. After validation, we performed global sensitivity and robustness analysis to estimate which parameters and species controlled model performance. These analyses suggested complement was robust to any single therapeutic intervention. The only intervention that consistently reduced C5a formation for all cases was a dual-knockdown of both C3 and C5. Taken together, we developed a reduced order complement model that was computationally inexpensive, and could easily be incorporated into pre-existing or new pharmacokinetic models of immune system function. The model described experimental data, and predicted the need for multiple points of therapeutic intervention to disrupt complement activation.

Keywords: Complement system, systems biology, reduced order models, biochemical engineering

1 Introduction

2 Complement is an important pathway in innate immunity. It plays a significant role in
3 inflammation, host defense as well as many disease processes. Complement was dis-
4 covered in the late 1880s where it was found to 'complement' the bactericidal activity of
5 natural antibodies (1). However, research over the past decade has shown that the im-
6 portance of complement extends well beyond innate immunity. For example, complement
7 contributes to tissue homeostasis by inducing tissue repair (2). Complement has also
8 been linked with several diseases including Alzheimers, Parkinson's disease, multiple
9 sclerosis, schizophrenia, rheumatoid arthritis and sepsis (3, 4). Complement plays both
10 positive and negative roles in cancer; attacking tumor cells with altered surface proteins
11 in some cases, while potentially contributing to tumor growth in others (5, 6). Lastly, sev-
12 eral other important biochemical subsystems are integrated with complement including
13 the coagulation cascade, the autonomous nervous system and inflammation (6). Thus,
14 complement is important in a variety of beneficial and potentially harmful functions in the
15 body.

16 The complement cascade involves over 30 soluble and cell surface proteins, receptors
17 and regulators. The molecular connectivity of complement is complex, see the review of
18 Walport (7, 8). The central outputs of complement are the Membrane Attack Complex
19 (MAC), and the inflammatory mediator proteins C3a and C5a. The membrane attack
20 complex, generated during the terminal phase of the response, forms transmembrane
21 channels which disrupt the membrane integrity of targeted cells, leading to cell lysis and
22 death. On the other hand, the C3a and C5a proteins act as a bridge between innate and
23 adaptive immunity, and play an important role in regulating inflammation (5). Complement
24 activation takes places through three pathways: the classical, the lectin binding and the
25 alternate pathways. Each of these pathways involves a different initiator signal which trig-
26 gers downstream events in the complement system. The classical pathway is triggered

27 by antibody recognition of foreign antigens or other pathogens. A multimeric protein com-
28 plex C1 binds to antibody-antigen complexes and undergoes a conformational change,
29 leading to an activated form with proteolytic activity. This activated complex then cleaves
30 soluble complement proteins C4 and C2 into C4a, C4b, C2a and C2b, respectively. The
31 C4a and C2b fragments bind to form the C4bC2a protease, which is also known as the
32 classical C3 convertase. The lectin pathway is initiated through the binding of L-ficolin or
33 Mannose Binding Lectin (MBL) to carbohydrates on the surfaces of bacterial pathogens.
34 These complexes, in combination with the associated mannose-associated serine pro-
35 teases 1 and 2 (MASP-1/2), also cleave C4 and C2, leading to additional classical C3
36 convertase. Thus, the classical and lectin pathways, initiated by the recognition of a for-
37 eign surface, converge at the classical C3 convertase. However, the alternate pathway
38 works differently. The alternate pathway involves a 'tickover' mechanism in which com-
39 plement protein C3 is spontaneously hydrolyzed to form an activated intermediate C3w;
40 C3w recruits factor B and factor D, leading to the formation of C3wBb. C3wBb can cleave
41 C3 into C3a and C3b, where the C3b fragment can further recruit additional factor B and
42 factor D to form C3bBbC3b, which is also known as the alternate C3 convertase (9). The
43 role of classical and alternate C3 convertases is varied. First, C3 convertases encode
44 an amplification loop by cleaving C3 into C3a and C3b; the C3b fragment is then free to
45 form additional alternate C3 convertases, thereby forming a positive feedback loop. Next,
46 C3 convertase activity links complement initiation with the terminal phase of the cascade
47 through the formation of C5 convertases. Both classical and alternate C3 convertases
48 can recruit an additional C3b subunit to form the classical C5 convertase (C4bC2aC3b),
49 and the alternate C5 convertase (C3bBbC3b), respectively. C5 convertases cleave C5
50 into the C5a and C5b fragments. The C5b fragment, along with the C6, C7, C8 and mul-
51 tiple C9 complement proteins, form the membrane attack complex. On the other hand,
52 both C3a and C5a are important inflammatory signals involved in several responses.

Activation of the complement cascade is strongly regulated by many plasma and host cell proteins. The initiation of the classical pathway via complement protein C1 is controlled by the C1 Inhibitor (C1-Inh), a protease inhibitor belonging to the serpin superfamily. C1-Inh irreversibly binds to and deactivates the active subunits of C1, preventing spontaneous fluid phase and chronic activation of complement (10). Regulation of the upstream elements of complement is also achieved through the interaction of the C4 binding protein (C4BP) with C4b, as well as through the interaction of factor H with C3b (11). These regulatory proteins are also capable of binding their respective targets while they are bound in convertase complexes. Membrane cofactor protein (MCP or CD46) possesses a cofactor activity for C4b and C3b, which protects the host from self-activation of complement (12). Decay accelerating factor (DAF or CD55) is also able to recognize and dissociate both C3 and C5 convertases (13). Carboxypeptidase-N, a well known inflammation regulator, cleaves carboxyl-terminal arginines and lysines of the complement proteins C3a, C4a, and C5a rendering them inactive (14). Lastly, the assembly of the MAC complex is inhibited by vitronectin and clusterin in the plasma, and CD59 at the host surface (15, 16). Thus, there are many points of control which influence complement activation across the three activation pathways.

Developing quantitative mathematical models of complement could be crucial to understanding its role in the body. Traditionally, complement models have been formulated as systems of linear or non-linear ordinary differential equations (ODEs). For example, Hirayama et al. modeled the classical complement pathway as a system of linear ODEs (17), while Korotaevskiy and co-workers modeled the classical, lectin and alternate pathways as a system of non-linear ODEs (18). More recently, large mechanistic models of sections of complement have also been proposed. For example, Liu et al. analyzed the formation of the classical and lectin C3 convertases, and the regulatory role of C4BP using a system of 45 non-linear ODEs with 85 parameters (19). Recently, Zewde and co-

79 workers constructed a detailed mechanistic model of the alternative pathway which con-
80 sisted of 107 ODEs and 74 kinetic parameters and delineated the complement response
81 of the host and pathogen (16). However, these previous modeling studies involved little
82 experimental validation. Thus, while these models are undoubtably important theoretical
83 tools, it is unclear if they can describe or quantitatively predict experimentally validated
84 complement dynamics. The central challenge is the estimation of model parameters from
85 experimental data. Unlike other important cascades, such as coagulation for which there
86 are well developed experimental tools and many publicly available data sets, the data for
87 complement is relatively sparse. Missing or incomplete data sets, and limited quantitative
88 data make the identification of mechanistic complement models difficult.

89 In this study, we developed an ensemble of experimentally validated reduced order
90 complement models. The modeling approach combined ordinary differential equations
91 with logical rules to produce a complement model with a limited number of equations and
92 parameters. The reduced order model, which described the lectin and alternative path-
93 ways, consisted of 18 differential equations with 28 parameters. Thus, the model was an
94 order of magnitude smaller and included more pathways than comparable mathematical
95 models in the literature. We estimated an ensemble of model parameters from *in vitro*
96 time series measurements of the C3a and C5a complement proteins. Subsequently, we
97 validated the model on unseen C3a and C5a measurements that were not used for model
98 training. Despite its small size, the model was surprisingly predictive. After validation, we
99 performed global sensitivity and robustness analysis to estimate which parameters and
100 species controlled model performance. These analyses suggested complement was ro-
101 bust to any single therapeutic intervention. The only intervention that consistently reduced
102 C5a formation for all cases was a dual-knockdown of both C3 and C5. Taken together,
103 we developed a reduced order complement model that was computationally inexpensive,
104 and could easily be incorporated into pre-existing or new pharmacokinetic models of im-

¹⁰⁵ immune system function. The model described experimental data, and predicted the need
¹⁰⁶ for multiple points of intervention to disrupt complement activation.

107 **Results**

108 **Reduced order complement network.** The complement model described the alternate
109 and lectin pathways (Fig. 1). A trigger event initiated the lectin pathway, which activated
110 the cleavage of C2 and C4 into C2a, C2b, C4a and C4b respectively. Classical Pathway
111 (CP) C3 convertase (C4aC2b) then catalyzed the cleavage of C3 into C3a and C3b. The
112 alternate pathway was initiated through the spontaneous hydrolysis of C3 into C3a and
113 C3b (not C3w). The C3b fragment generated by hydrolysis (or by CP C3 convertase)
114 could then form the alternate pathway (AP) C3 convertase (C3bBb). We did not consider
115 C3w, nor the formation of the initial alternate C3 convertase (C3wBb). Rather, we as-
116 sumed C3w was equivalent to C3b and only modeled the formation of the main AP C3
117 convertase. Both the CP and AP C3 convertases catalyzed the cleavage of C3 into C3a
118 and C3b. A second C3b fragment could then bind with either the CP or AP C3 convertase
119 to form the CP or AP C5 convertase (C4bC2aC3b or C3bBbC3b). Both C5 convertases
120 catalyzed the cleavage of C5 into the C5a and C5b fragments. In this initial study, we
121 simplified the model by assuming both Factor B and Factor D were in excess. However,
122 we did explicitly account for two control proteins, Factor H and C4BP. Lastly, we did not
123 consider MAC formation, instead we stopped at C5a and C5b. Lectin pathway activation,
124 and C3/C5 convertase activity was modeled using a combination of saturation kinetics
125 and non-linear transfer functions, which facilitated a significant reduction in the size of the
126 model while maintaining performance. Binding interactions were modeled using mass-
127 action kinetics, where we assumed all binding was irreversible. Thus, while the reduced
128 order complement model encoded significant biology, it was highly compact consisting of
129 only 18 differential equations and 28 model parameters. Next, we estimated an ensemble
130 of model parameters from time series measurements of the C3a and C5a complement
131 proteins.

132 **Estimating an ensemble of reduced order complement models.** A critical challenge
133 for any dynamic model is the estimation of model parameters. We estimated the com-
134 plement model parameters in a hierarchical fashion using two *in vitro* time-series data
135 sets generated with and without zymosan, a lectin pathway activator (20). The residual
136 between model simulations and experimental measurements was minimized using the dy-
137 namic optimization with particle swarms (DOPS) approach, starting from an initial random
138 parameter guess. A hierarchical approach was taken to determine model parameters in
139 which the alternate pathway parameters were first estimated and then fixed during the
140 estimation of the lectin pathway parameters. The reduced order complement model cap-
141 tured the behavior of the alternative and lectin pathways (Fig. 2). For the alternative
142 pathway, we used the C3a and C5a measurements in the absence of zymosan, and only
143 allowed the alternative parameters to vary (Fig. 2A and B). Lectin parameters were es-
144 timated from C3a and C5a measurements in the presence of 1g zymosan (Fig. 2C and
145 D). Taken together, the reduced order model reproduced a panel of lectin pathway initi-
146 ation data sets in the neighborhood of physiological factor and inhibitor concentrations.
147 However, it was unclear whether the reduced order model could predict new data, without
148 updating the model parameters. To address this question, we fixed the model parameters
149 and simulated data not used for model training.

150 We tested the predictive power of the reduced order complement model with data not
151 used during model training (Fig. 3). Six validation cases were considered, three for C3a
152 and C5a respectively at different zymosan concentrations. All model parameters were
153 fixed for the validation simulations. The ensemble of reduced order models captured the
154 qualitative dynamics of C3a formation (Fig. 3, left column), and C5a formation (Fig. 3,
155 right column) at three inducer concentrations. However, there were shortcomings, espe-
156 cially for the C3a prediction. First, while the C3a dynamics and concentration peak times
157 were captured, the overall level of C3a was under-predicted in all cases (Fig. 3, inset

left column). We believe the C3a under-prediction can be attributed to how we modeled C4BP interactions. C4BP interactions were modeled as irreversible binding steps resulting in completely inactive complexes; however, the binding of C4BP with complement proteins is likely reversible and convertases may have residual activity even in the bound form. Thus, the model may over-predict the influence of C4BP. We also failed to capture the concave down curvature for the 0.001 g and 0.01 g zymosan cases in the C5a validation studies. The decreasing slope of the C5a measurements may indicate decreasing cofactors abundance, or missing biology which we have not explicitly accounted for in the reduced order approach. However, despite these shortcomings, we qualitatively predicted unseen experimental data, including correctly capturing the dynamic time scale of C3a formation, and the correct order of magnitude for the concentration of C5a for three inducer levels. Next, we used global sensitivity and robustness analysis to determine which parameters and species controlled the performance of the complement model.

Global analysis of the reduced order complement model We conducted sensitivity analysis to estimate which parameters controlled the performance of the reduced order complement model. We calculated the sensitivity of the C3a and C5a residuals with and without zymosan for the ensemble of parameter sets (Fig. 4A - D). In the absence of zymosan (where only the alternative pathway is active), $k_{f,C3b}$ (formation of C3b) and $k_{d,C3a}$ (degradation rate constant governing C3a) were largely responsible for the system response. Interestingly, $k_{c,C3}$ (the rate constant governing AP C3-convertase activity) was not sensitive in the absence of zymosan. Thus, the behavior of the alternative pathway was more heavily influenced by the spontaneous hydrolysis of C3, rather than AP C3-convertase activity. On the other hand, $k_{c,C3}$ was one of the parameters that controlled C5a formation, in addition to the expected parameters related to AP C5-convertase formation. The AP C3-convertase is required for AP C5-convertase formation, and the formation of the C3b fragment. Thus, changes in the activity of AP C3-convertase will not

184 drastically change the C3a dynamics, but will effect AP C5-convertase activity and C5a
185 formation. The sensitivity analysis yielded the expected results for the lectin pathway that
186 included parameters sensitive to pathway initiation (Fig. 4C and D). One key difference
187 observed between the sensitivity of C3a and C5a parameters, was their respective degra-
188 dation constants. The rate constant governing C3a degradation was sensitive, while the
189 degradation constant for C5a was not. This difference was likely attributable to the mag-
190 nitude of the degradation parameters and the respective concentrations of C3a and C5a.
191 Thus, sensitivity analysis identified important indirect parameter interactions that could
192 have therapeutic significance. However, sensitivity coefficients are a local measure of
193 how small changes in a parameter value effects a performance objective, for example the
194 abundance of C5a. To more closely simulate a clinical intervention e.g., administration of
195 an anti-complement antibody, we performed robustness analysis. Robustness coefficients
196 quantify the response of a marker to a macroscopic structural or operational perturbation
197 to the network architecture. In this case, we computed how the C3a and C5a trajectories
198 responded to a decrease in the initial abundance of C3 and C5.

199 Robustness analysis suggested there was no single intervention that inhibited com-
200 plement activation in the presence of both initiation pathways (Fig. 5). We calculated
201 robustness indices for C3a and C5a for the 50 parameter sets in the ensemble with and
202 without the lectin pathway initiator. We simulated the addition of different doses of anti-
203 complement antibody cocktails by decreasing the initial concentration of C3 or C5 or the
204 combination of C3 and C5 by 50% and 90%. A \log_{10} transformed robustness index of
205 zero indicated no effect due to the perturbation, whereas an index of less than zero in-
206 dicated decreased C3a or C5a. As expected, a C5 knockdown had no effect on C3a
207 formation for either the alternate (Fig. 5A, lanes 1 or 3) or lectin pathways (Fig. 5B, lanes
208 1 or 3). However, C3a abundance and to a lesser extent C5a abundance decreased with
209 decreasing C3 concentration in the alternate pathway (Fig. 5A or B, lanes 1 or 2). This

210 agreed with the sensitivity results; changes in AP C3-convertase formation or activity af-
211 fected the downstream dynamics of C5a formation. Thus, these results suggested that C3
212 alone would be a reasonable target, especially given that C5a formation was surprisingly
213 robust to C5 levels in the alternate pathway (Fig. 5A or B, lane 2). Yet, in lectin initiated
214 complement activation, C5a levels were robust to the initial C3 concentration (Fig. 5A or
215 B, lane 4). Thus, above some limiting threshold, even small concentrations of C3 and C5
216 convertases catalyzed the downstream formation of C5a. The only reliable intervention
217 that consistently reduced C5a formation for all cases was a dual-knockdown. For exam-
218 ple, a 90% decrease of both C3 and C5 reduced the formation of C5a by over an order of
219 magnitude (Fig. 5B, lane 4).

220 **Discussion**

221 In this study, we developed an ensemble of experimentally validated reduced order com-
222 plement models. The modeling approach combined ordinary differential equations with
223 logical rules to produce a complement model with a limited number of equations and pa-
224 rameters. The reduced order model, which described the lectin and alternative pathways,
225 consisted of 18 differential equations with 28 parameters. Thus, the model was an order
226 of magnitude smaller and included more pathways than comparable mathematical mod-
227 els in the literature. We estimated an ensemble of model parameters from *in vitro* time
228 series measurements of the C3a and C5a complement proteins. Subsequently, we val-
229 idated the model on unseen C3a and C5a measurements that were not used for model
230 training. Despite its small size, the model was surprisingly predictive. After validation, we
231 performed global sensitivity and robustness analysis to estimate which parameters and
232 species controlled model performance. These analyses suggested complement was ro-
233 bust to any single therapeutic intervention. The only intervention that consistently reduced
234 C5a formation for all cases was a dual-knockdown of both C3 and C5. Taken together,
235 we developed a reduced order complement model that was computationally inexpensive,
236 and could easily be incorporated into pre-existing or new pharmacokinetic models of im-
237 mune system function. The model described experimental data, and predicted the need
238 for multiple points of intervention to disrupt complement activation.

239 Despite its importance, there has been a paucity of validated mathematical models
240 of complement pathway activation. To our knowledge, this study is one of the first com-
241 plement models that combined multiple initiation pathways with experimental validation
242 of important complement products like C5a. However, there have been several theoreti-
243 cal models of components of the cascade in the literature. Liu and co-workers modeled
244 the formation of C3a through the classical pathway using 45 non-linear ODEs (19). In
245 contrast, in this study we modeled lectin mediated C3a formation using only five ODEs.

246 Though we did not model all the initiation interactions in detail, especially the cross-talk
247 between the lectin and classical pathways, we successfully captured C3a dynamics with
248 respect to different concentrations of lectin initiators. The model also captured the dy-
249 namics of C3a and C5a formed from the alternate pathway using only seven ODEs. The
250 reduced order model predictions of C5a were qualitatively similar to the theoretical com-
251 plement model of Zewde et al which involved over 100 ODEs (16). However, we found
252 that the quantity of C3a produced in the alternate pathway was nearly 1000 times the
253 quantity of C5a produced. Though this was in agreement with the experimental data (20),
254 it differed from the theoretical predictions made by Zewde et al. who showed C3a was 10^8
255 times the C5a concentration (16). In our model, the time profile of C5a generation from the
256 lectin pathway changed with respect to the quantity of zymosan (the lectin pathway initia-
257 tor). The lag phase for generation was inversely proportional to the initiator concentration.
258 Korotaevskiy et al. showed a similar trend using a theoretical model of complement, albeit
259 for much shorter time scales (18). Thus, the reduced order complement model performed
260 similarly to existing large mechanistic models, despite being significantly smaller.

261 Global analysis of the complement model estimated potential important therapeutic
262 targets. Complement malfunctions are implicated in a number of diseases, however the
263 development of complement specific therapeutics has been challenging (3, 21). Previ-
264 ously, we have shown that mathematical modeling and sensitivity analysis can be useful
265 tools to estimate therapeutically important mechanisms in biochemical networks (22–25).
266 In this study, we analyzed a validated ensemble of reduced order complement models to
267 estimate therapeutically important mechanisms. In presence of an initiator, C5a forma-
268 tion was primarily sensitive to the lectin initiation parameters, and parameters governing
269 the conversion of C5 to C5a and C5b. This result agrees well with the current protease
270 inhibitors targeting initiating complexes, including mannose-associated serine proteases
271 1 and 2 (MASP-1,2) (26). The most commonly used anti-complement drug eculizumab

272 (21), targets the C5 protein which is cleaved to form C5a. Our sensitivity analysis showed
273 that kinetic parameters governing C5 conversion were sensitive in both lectin initiated and
274 alternate pathways, thus agreeing with targeting C5 protein. The formation of basal C3b
275 was also a sensitive parameter in the formation of C3a through the alternate pathway.
276 Thus, this mechanism can act as a target for both C3a and C5a inhibitors. Lectin initiated
277 C3a formation showed a number of sensitive parameters. This included the lectin initi-
278 ation parameters that controlled C5a formation, C3 convertase inhibition by C4BP, and
279 parameters governing C3 convertase activity. All these mechanisms are potential drug
280 targets.

281 To further validate these results from sensitivity analysis about potential drug targets
282 we did a robustness analysis. We knocked down C3 and C5 levels and studied their im-
283 pact on the generation of C3a and C5a. The C3a and C5a levels in the lectin pathway
284 were strongly influenced by initial levels of C3 and C5. Thus direct inhibition of C3 and
285 C5, or targeting complexes (MASP complex, C3 and C5 convertases) that act on C3 and
286 C5 have a direct impact on production of C3a and C5a. This is also in agreement with
287 sensitivity analysis that C5 is a good drug target. A number of drugs targeting C5 are
288 being developed. For example LFG316 by Novartis is being used to target C5 in cases
289 of Age-Related Macular Degeneration (27), Mubodina is an antibody that targets C5 in
290 the treatment of Atypical Hemolytic-Uremic Syndrome (aHUS) (28), Coversin is a small
291 molecule targeting C5 (29), Zimura is an aptamer targeting C5 (30), small peptides and
292 RNAi are also being used to inhibit C5 (31). Another important conclusion that can be
293 drawn together from sensitivity and robustness analysis is that C3 and C5 convertases
294 can be important therapeutic targets. Though knockdown of C3 and C5 affects C3a and
295 C5a levels downstream, the abundance and turnover rate (32, 33) of these proteins make
296 them difficult targets. Thus targeting C3 and C5 directly will require high dosage of drugs.
297 It is also well known that eculizumab dosage needs to be adjusted while treating for Atyp-

ical Hemolytic-Uremic Syndrome (aHUS), a disease that is caused due to uncontrolled complement activation (34). The issue of high dosage can potentially be circumvented by targeting convertases or fragile mechanisms that involve C3, C5 or their activated components. Our analysis shows that formation and assembly of these convertases are sensitive mechanisms that strongly impact downstream proteins like C5a. Formation of convertases is inhibited by targeting upstream protease complexes like MASP-1,2 from lectin pathway (or C1r, C1s from classical pathway). For example, Omeros is a protease inhibitor that targets MASP-2 complex and thereby inhibits formation of downstream convertases (35). Lampalizumab (an immunoglobulin) and Bikaciomab (an antibody fragment) target Factor B and Factor D respectively. Factor B and Factor D are crucial to formation alternate pathway convertases (36, 37). Novelmed Therapeutics recently developed antibody, NM9401 against propedin, a small protein that stabilizes alternate C3 convertase (38). Cobra Venom Factor (CVF), an analogue of C3b has been used to bind to Factor B to regulate alternate convertases (39). Thus, analysis of the ensemble of complement models identified potentially important therapeutic targets that are consistent with therapeutic strategies that are under development.

The performance of the complement model was impressive given its limited size. However, there are several questions that should be explored further. A logical progression for this work would be to expand the network to include the classical pathway and the formation of the membrane attack complex (MAC). However, it is unclear whether the addition of the classical pathway will decrease the predictive quality of our existing model. Liu et al have shown cross-talk between the activation of the classical and lectin pathways that could influence model performance (19). One potential approach to address such difficulties would be to incorporate C reactive proteins (CRP) and L-ficolin (LF) into the model, both of which are involved with the initiation of classical and lectin pathways. Liu et al. showed that under inflammation conditions interactions between lectin and classical

pathways was mediated through CRP and LF (19). Thus incorporating these two proteins would help us in modeling cross talk. Time course measurements of MAC abundance (and MAC formation dynamics) are also scarce, making the inclusion of MAC challenging. Next, we should address the under-prediction of C3a. We believe the C3a under-prediction can be attributed to how we modeled C4BP interactions. C4BP interactions were modeled as irreversible binding steps resulting in completely inactive complexes; however, the binding of C4BP with complement proteins is likely reversible and C4BP-bound convertases may have residual activity. We also did not capture the maximum concentration of C3a at low initiator levels. One possible reasons for this could be the C2-by-pass pathway, which was not included in the model. This pathway further accelerates C3a production without the involvement of a C3 convertase. Currently the C3a in the model is generated only through the activity of a C3 convertase. Incorporating this additional step within the reduced order modeling framework would be a future direction that we need to consider. We should test alternative model structures which include reversible C4BP binding, and partially active convertases. Alternatively, we could also perform sensitivity analysis on the C3a prediction residual to determine which parameters controlled the C3a prediction.

341 **Materials and Methods**

342 **Formulation and solution of the complement model equations.** We used ordinary
 343 differential equations (ODEs) to model the time evolution of complement proteins (x_i) in
 344 the reduced order model:

$$\frac{dx_i}{dt} = \sum_{j=1}^{\mathcal{R}} \sigma_{ij} r_j(\mathbf{x}, \epsilon, \mathbf{k}) \quad i = 1, 2, \dots, \mathcal{M} \quad (1)$$

345 where \mathcal{R} denotes the number of reactions and \mathcal{M} denotes the number of protein species
 346 in the model. The quantity $r_j(\mathbf{x}, \epsilon, \mathbf{k})$ denotes the rate of reaction j . Typically, reaction j is
 347 a non-linear function of biochemical and enzyme species abundance, as well as unknown
 348 model parameters \mathbf{k} ($\mathcal{K} \times 1$). The quantity σ_{ij} denotes the stoichiometric coefficient for
 349 species i in reaction j . If $\sigma_{ij} > 0$, species i is produced by reaction j . Conversely, if $\sigma_{ij} < 0$,
 350 species i is consumed by reaction j , while $\sigma_{ij} = 0$ indicates species i is not connected
 351 with reaction j . Species balances were subject to the initial conditions $\mathbf{x}(t_0) = \mathbf{x}_0$.

352 Rate processes were written as the product of a kinetic term (\bar{r}_j) and a control term
 353 (v_j) in the complement model. The kinetic term for the formation of C4a, C4b, C2a and
 354 C2b, lectin pathway activation, and C3 and C5 convertase activity was given by:

$$\bar{r}_j = k_j^{max} \epsilon_i \left(\frac{x_s^\eta}{K_{js}^\eta + x_s^\eta} \right) \quad (2)$$

355 where k_j^{max} denotes the maximum rate for reaction j , ϵ_i denotes the abundance of the
 356 enzyme catalyzing reaction j , η denotes a cooperativity parameter, and K_{js} denotes the
 357 saturation constant for species s in reaction j . We used mass action kinetics to model
 358 protein-protein binding interactions within the network:

$$\bar{r}_j = k_j^{max} \prod_{s \in m_j^-} x_s^{-\sigma_{sj}} \quad (3)$$

359 where k_j^{max} denotes the maximum rate for reaction j , σ_{sj} denotes the stoichiometric co-
 360 efficient for species s in reaction j , and $s \in m_j$ denotes the set of *reactants* for reaction
 361 j . We assumed all binding interactions were irreversible. The control terms $0 \leq v_j \leq 1$
 362 depended upon the combination of factors which influenced rate process j . For each rate,
 363 we used a rule-based approach to select from competing control factors. If rate j was in-
 364 fluenced by $1, \dots, m$ factors, we modeled this relationship as $v_j = \mathcal{I}_j(f_{1j}(\cdot), \dots, f_{mj}(\cdot))$
 365 where $0 \leq f_{ij}(\cdot) \leq 1$ denotes a regulatory transfer function quantifying the influence of
 366 factor i on rate j . The function $\mathcal{I}_j(\cdot)$ is an integration rule which maps the output of regu-
 367 latory transfer functions into a control variable. Each regulatory transfer function took the
 368 form:

$$f_{ij}(\mathcal{Z}_i, k_{ij}, \eta_{ij}) = k_{ij}^{\eta_{ij}} \mathcal{Z}_i^{\eta_{ij}} / (1 + k_{ij}^{\eta_{ij}} \mathcal{Z}_i^{\eta_{ij}}) \quad (4)$$

369 where \mathcal{Z}_i denotes the abundance of factor i , k_{ij} denotes a gain parameter, and η_{ij} denotes
 370 a cooperativity parameter. In this study, we used $\mathcal{I}_j \in \{min, max\}$ (40). If a process has
 371 no modifying factors, $v_j = 1$. The model equations were implemented in MATLAB and
 372 solved using the ODE23s routine (The Mathworks, Natick MA). The complement model
 373 code and parameter ensemble is freely available under an MIT software license and can
 374 be downloaded from <http://www.varnerlab.org>.

375 **Estimation of an ensemble of complement model parameters.** We minimized the
 376 residual between simulations and experimental C3a and C5a measurements using Dy-
 377 namic Optimization with Particle Swarms (DOPS). DOPS minimized the objective:

$$\min_{\mathbf{k}} \sum_{\tau=1}^{\mathcal{T}} \sum_{j=1}^S \left(\frac{\hat{x}_j(\tau) - x_j(\tau, \mathbf{k})}{\omega_j(\tau)} \right)^2 \quad (5)$$

378 where $\hat{x}_j(\tau)$ denotes the measured value of species j at time τ , $x_j(\tau, \mathbf{k})$ denotes the sim-
 379 ulated value for species j at time τ , and $\omega_j(\tau)$ denotes the experimental measurement

variance for species j at time τ . The outer summation is with respect to time, while the inner summation is with respect to state. DOPS is a novel metaheuristic that combines multi swarm particle swarm optimization (PSO) with a greedy global optimization algorithm called dynamically dimensioned search (DDS). DOPS is faster than conventional global optimizers and has the ability to find near optimal solutions for high dimensional systems within a relatively few function evaluations. It uses an adaptive switching strategy based on error convergence rates to switch from the particle swarm to DDS search phases. This enables DOPS to quickly estimate globally optimal or near optimal solutions even in the presence of many local minima. In the swarm search, for each iteration the particles compute error within each sub-swarm by evaluating the model equations using their specific parameter vector realization. From each of these points within a sub-swarm a local best is identified. This along with the particle best within the sub-swarm S_k is used to update the parameter estimate for each particle using the following rules:

$$z_{i,j} = \theta_1 z_{i,j-1} + \theta_2 r_1 (\mathcal{L}_i - z_{i,j-1}) + \theta_3 r_2 (\mathcal{G}_k - z_{i,j-1}) \quad (6)$$

where $z_{i,j}$ is the parameter vector, $(\theta_1, \theta_2, \theta_3)$ were adjustable parameters, \mathcal{L}_i denotes the best solution found by particle i within sub-swarm S_k for function evaluations $1 \rightarrow j-1$, and \mathcal{G}_k denotes the best solution found over all particles within sub-swarm S_k . The quantities r_1 and r_2 denote uniform random vectors with the same dimension as the number of unknown model parameters ($K \times 1$). At the conclusion of the swarm phase, the overall best particle, \mathcal{G}_k , over the k sub-swarms was used to initialize the DDS phase. For the DDS phase, the best parameter estimate was updated using the rule:

$$\mathcal{G}_{new}(J) = \begin{cases} \mathcal{G}(J) + \mathbf{r}_{normal}(J)\sigma(J), & \text{if } \mathcal{G}_{new}(J) < \mathcal{G}(J). \\ \mathcal{G}(J), & \text{otherwise.} \end{cases} \quad (7)$$

400 where \mathbf{J} is a vector representing the subset of dimensions that are being perturbed, \mathbf{r}_{normal}
401 denotes a normal random vector of the same dimensions as \mathcal{G} , and σ denotes the pertur-
402 bation amplitude:

$$\sigma = R(\mathbf{p}^U - \mathbf{p}^L) \quad (8)$$

403 where R is the scalar perturbation size parameter, \mathbf{p}^U and \mathbf{p}^L are $(\mathcal{K} \times 1)$ vectors that
404 represent the maximum and minimum bounds on each dimension. The set \mathbf{J} was con-
405 structed using a monotonically decreasing probability function \mathcal{P}_i that represents a thresh-
406 old for determining whether a specific dimension j was perturbed or not. DDS updates
407 are greedy; \mathcal{G}_{new} becomes the new solution vector only if it is better than \mathcal{G} . At the end of
408 DDS phase we obtain the optimal vector \mathcal{G} which we use for plotting best fits against the
409 experimental data, and for generating a parameter ensemble.

410 An ensemble of parameters was obtained by randomly perturbing the optimal param-
411 eter set within bounds established by perturbing each parameter and measuring the in-
412 crease in the residual. Thereafter, the optimal parameter vector was perturbed within
413 these bounds for approximately 100,000 iterations. Within each iteration the quality of
414 perturbed vector was measured using goodness of fit (model residual). If the residual was
415 too high or the perturbed vector generated a numerical error, the vector was rejected. We
416 selected an ensemble of $N = 50$ parameter sets for this study using this sampling proce-
417 dure. The DOPS routine was implemented in MATLAB (The Mathworks, Natick MA) and
418 can be downloaded from <http://www.varnerlab.org> under an MIT software license.

419 **Sensitivity and robustness analysis of complement model performance.** We con-
420 ducted global sensitivity and robustness analysis to estimate which parameters and species
421 controlled the performance of the reduced order model. We computed the total variance-
422 based sensitivity index of each parameter relative to the training residual for the C3a
423 alternate, C5a alternate, C3a lectin, and C5a lectin cases using the Sobol method (41).

424 The sampling bounds for each parameter were established from the minimum and maxi-
 425 mum value for that parameter in the parameter ensemble. We used the sampling method
 426 of Saltelli *et al.* to compute a family of $N(2d + 2)$ parameter sets which obeyed our pa-
 427 rameter ranges, where N was the number of trials per parameters, and d was the number
 428 of parameters in the model (42). In our case, $N = 200$ and $d = 28$, so the total sensitivity
 429 indices were computed using 11,600 model evaluations. The variance-based sensitivity
 430 analysis was conducted using the SALib module encoded in the Python programming
 431 language (43).

432 Robustness coefficients quantify the response of a marker to a structural or operational
 433 perturbation to the network architecture. Robustness coefficients were calculated as
 434 shown previously (44). Log-transformed robustness coefficients denoted by $\hat{\alpha}(i, j, t_o, t_f)$
 435 are defined as:

$$\hat{\alpha}(i, j, t_o, t_f) = \log_{10} \left[\left(\int_{t_o}^{t_f} x_i(t) dt \right)^{-1} \left(\int_{t_o}^{t_f} x_i^{(j)}(t) dt \right) \right] \quad (9)$$

436 Here t_o and t_f denote the initial and final simulation time, while i and j denote the indices
 437 for the marker and the perturbation, respectively. A value of $\hat{\alpha}(i, j, t_o, t_f) > 0$, indicates
 438 increased marker abundance, while $\hat{\alpha}(i, j, t_o, t_f) < 0$ indicates decreased marker abun-
 439 dance following perturbation j . If $\hat{\alpha}(i, j, t_o, t_f) \sim 0$, perturbation j did not influence the
 440 abundance of marker i . In this study, we perturbed the initial condition of C3 or C5 or
 441 a combination of C3 and C5 by 50% or 90% and measured the area under the curve
 442 (AUC) of C3a or C5a with and without lectin initiator. Log-transformed robustness coeffi-
 443 cients were calculated for every member of the ensemble, where the mean $\pm 1 \times$ standard-
 444 deviation are reported.

⁴⁴⁵ **Competing interests**

⁴⁴⁶ The authors declare that they have no competing interests.

⁴⁴⁷ **Author's contributions**

⁴⁴⁸ J.V directed the study. A.S developed the reduced order complement model and the
⁴⁴⁹ parameter ensemble. A.S, W.D and M.M analyzed the model ensemble, and generated
⁴⁵⁰ figures for the manuscript. The manuscript was prepared and edited for publication by
⁴⁵¹ A.S, W.D, M.M and J.V.

⁴⁵² **Acknowledgements**

⁴⁵³ We gratefully acknowledge the suggestions from the anonymous reviewers to improve
⁴⁵⁴ this manuscript.

⁴⁵⁵ **Funding**

⁴⁵⁶ This study was supported by an award from the US Army and Systems Biology of Trauma
⁴⁵⁷ Induced Coagulopathy (W911NF-10-1-0376) to J.V. for the support of A.S.

458 **References**

- 459 1. Nuttall G (1888) Experimente über die bacterienfeindlichen Einflüsse des thierischen
460 Körpers. *Z Hyg Infektionskr* 4: 353-394.
- 461 2. Ricklin D, Hajishengallis G, Yang K, Lambris JD (2010) Complement: a key system
462 for immune surveillance and homeostasis. *NAT IMMUNOL* 11: 785–797.
- 463 3. Ricklin D, Lambris JD (2007) Complement-targeted therapeutics. *NAT BIOTECHNOL*
464 25: 1265-1275.
- 465 4. Rittirsch D, Flierl MA, Ward PA (2008) Harmful molecular mechanisms in sepsis. *NAT*
466 *REV IMMUNOL* 8: 776–787.
- 467 5. Sarma JV, Ward PA (2011) The complement system. *Cell Tissue Res* 343: 227–235.
- 468 6. Ricklin D, Lambris JD (2013) Complement in immune and inflammatory disorders:
469 pathophysiological mechanisms. *J Immunol* 190: 3831–3838.
- 470 7. Walport MJ (2001) Complement. first of two parts. *N Engl J Med* 344: 1058-66.
- 471 8. Walport MJ (2001) Complement. second of two parts. *N Engl J Med* 344: 1140-4.
- 472 9. Pangburn MK, Müller-Eberhard HJ (1984) The alternative pathway of complement.
473 *Semin Immunopathol* .
- 474 10. Walker D, Yasuhara O, Patston P, McGeer E, McGeer P (1995) Complement c1 in-
475 hibitor is produced by brain tissue and is cleaved in alzheimer disease. *Brain Res*
476 675: 75–82.
- 477 11. Blom AM, Kask L, Dahlbäck B (2001) Structural requirements for the complement
478 regulatory activities of c4bp. *J Biol Chem* 276: 27136–27144.
- 479 12. Riley-Vargas RC, Gill DB, Kemper C, Liszewski MK, Atkinson JP (2004) Cd46: ex-
480 panding beyond complement regulation. *Trends Immunol* 25: 496–503.
- 481 13. Lukacik P, Roversi P, White J, Esser D, Smith G, et al. (2004) Complement regulation
482 at the molecular level: the structure of decay-accelerating factor. *Proc Natl Acad Sci*
483 *USA* 101: 1279–1284.

- 484 14. Liszewski MK, Farries TC, Lublin DM, Rooney IA, Atkinson JP (1995) Control of the
485 complement system. *Adv Immunol* 61: 201–283.
- 486 15. Chauhan A, Moore T (2006) Presence of plasma complement regulatory proteins
487 clusterin (apo j) and vitronectin (s40) on circulating immune complexes (cic). *Clin
488 Exp Immunol* 145: 398–406.
- 489 16. Zewde N, Gorham Jr RD, Dorado A, Morikis D (2016) Quantitative modeling of the
490 alternative pathway of the complement system. *PLoS one* 11: e0152337.
- 491 17. Hirayama H, Yoshii K, Ojima H, Kawai N, Gotoh S, et al. (1996) Linear systems analy-
492 sis of activating processes of complement system as a defense mechanism. *Biosys-
493 tems* 39: 173–185.
- 494 18. Korotaevskiy AA, Hanin LG, Khanin MA (2009) Non-linear dynamics of the comple-
495 ment system activation. *Math Biosci* 222: 127–143.
- 496 19. Liu B, Zhang J, Tan PY, Hsu D, Blom AM, et al. (2011) A computational and experi-
497 mental study of the regulatory mechanisms of the complement system. *PLoS Comput
498 Biol* 7: e1001059.
- 499 20. Morad HO, Belete SC, Read T, Shaw AM (2015) Time-course analysis of c3a and
500 c5a quantifies the coupling between the upper and terminal complement pathways in
501 vitro. *J Immunol Methods* 427: 13–18.
- 502 21. Morgan BP, Harris CL (2015) Complement, a target for therapy in inflammatory and
503 degenerative diseases. *NAT REV DRUG DISCOV* 14: 857-877.
- 504 22. Luan D, Zai M, Varner JD (2007) Computationally derived points of fragility of a human
505 cascade are consistent with current therapeutic strategies. *PLoS Comput Biol* 3:
506 e142.
- 507 23. Nayak S, Salim S, Luan D, Zai M, Varner JD (2008) A test of highly optimized tol-
508 erance reveals fragile cell-cycle mechanisms are molecular targets in clinical cancer
509 trials. *PLoS One* 3: e2016.

- 510 24. Tasseff R, Nayak S, Salim S, Kaushik P, Rizvi N, et al. (2010) Analysis of the molecular
511 networks in androgen dependent and independent prostate cancer revealed fragile
512 and robust subsystems. PLoS One 5: e8864.
- 513 25. Rice NT, Szlam F, Varner JD, Bernstein PS, Szlam AD, et al. (2016) Differential con-
514 tributions of intrinsic and extrinsic pathways to thrombin generation in adult, maternal
515 and cord plasma samples. PLoS One 11: e0154127.
- 516 26. Héja D, Harmat V, Fodor K, Wilmanns M, Dobó J, et al. (2012) Monospecific inhibitors
517 show that both mannan-binding lectin-associated serine protease-1 (masp-1) and-2
518 are essential for lectin pathway activation and reveal structural plasticity of masp-2. J
519 Biol Chem : 20290–20300.
- 520 27. Roguska M, Splawski I, Diefenbach-Streiber B, Dolan E, Etemad-Gilbertson B, et al.
521 (2014) Generation and characterization of Ifg316, a fully-human anti-c5 antibody for
522 the treatment of age-related macular degeneration. Investigative Ophthalmology &
523 Visual Science : 3433–3433.
- 524 28. Melis JP, Strumane K, Ruuls SR, Beurskens FJ, Schuurman J, et al. (2015) Com-
525 plement in therapy and disease: Regulating the complement system with antibody-
526 based therapeutics. Molecular immunology : 117–130.
- 527 29. Weston-Davies WH, Nunn MA, Pinto FO, Mackie IJ, Richards SJ, et al. (2014) Clin-
528 ical and immunological characterisation of coversin, a novel small protein inhibitor of
529 complement c5 with potential as a therapeutic agent in pnh and other complement
530 mediated disorders. Blood : 4280–4280.
- 531 30. Epstein D, Kurz JC (2007). Complement binding aptamers and anti-c5 agents useful
532 in the treatment of ocular disorders. US Patent App. 12/224,708.
- 533 31. Borodovsky A, Yucius K, Sprague A, Banda NK, Holers VM, et al. (2014) Aln-cc5, an
534 investigational rnai therapeutic targeting c5 for complement inhibition. Complement
535 20: 40.

- 536 32. Sissons J, Liebowitch J, Amos N, Peters D (1977) Metabolism of the fifth component
537 of complement, and its relation to metabolism of the third component, in patients with
538 complement activation. *J Clin Invest* 59: 704.
- 539 33. Swaak A, Hannema A, Vogelaar C, Boom F, van Es L, et al. (1982) Determination of
540 the half-life of c3 in patients and its relation to the presence of c3-breakdown products
541 and/or circulating immune complexes. *Rheumatol Int* : 161–166.
- 542 34. Noris M, Galbusera M, Gastoldi S, Macor P, Banterla F, et al. (2014) Dynamics of
543 complement activation in ahus and how to monitor eculizumab therapy. *Blood* : 1715–
544 1726.
- 545 35. Schwaeble HW, Stover CM, Tedford CE, Parent JB, Fujita T (2011). Methods for
546 treating conditions associated with masp-2 dependent complement activation. US
547 Patent 7,919,094.
- 548 36. Katschke KJ, Wu P, Ganesan R, Kelley RF, Mathieu MA, et al. (2012) Inhibiting al-
549 ternative pathway complement activation by targeting the factor d exosite. *Journal of*
550 *Biological Chemistry* : 12886–12892.
- 551 37. Hu X, Holers VM, Thurman JM, Schoeb TR, Ramos TN, et al. (2013) Therapeutic in-
552 hibition of the alternative complement pathway attenuates chronic eae. *Mol Immunol*
553 : 302–308.
- 554 38. Bansal R (2014). Humanized and chimeric anti-properdin antibodies. US Patent
555 8,664,362.
- 556 39. Vogel CW, Fritzinger DC, Hew BE, Thorne M, Bammert H (2004) Recombinant cobra
557 venom factor. *Molecular immunology* : 191–199.
- 558 40. Sagar A, Varner JD (2015) Dynamic modeling of the human coagulation cascade
559 using reduced order effective kinetic models. *Processes* 3: 178.
- 560 41. Sobol I (2001) Global sensitivity indices for nonlinear mathematical models and their
561 monte carlo estimates. *MATH COMPUT SIMULAT* 55: 271 - 280.

- 562 42. Saltelli A, Annoni P, Azzini I, Campolongo F, Ratto M, et al. (2010) Variance based
563 sensitivity analysis of model output. design and estimator for the total sensitivity index.
564 Comput Phys Commun 181: 259–270.
- 565 43. Herman J. Salib: Sensitivity analysis library in python (numpy). con-
566 tains sobol, morris, fractional factorial and fast methods. available online:
567 <https://github.com/jdherman/salib>.
- 568 44. Tasseff R, Nayak S, Song SO, Yen A, Varner JD (2011) Modeling and analysis
569 of retinoic acid induced differentiation of uncommitted precursor cells. Integr Biol
570 (Camb) 3: 578-91.

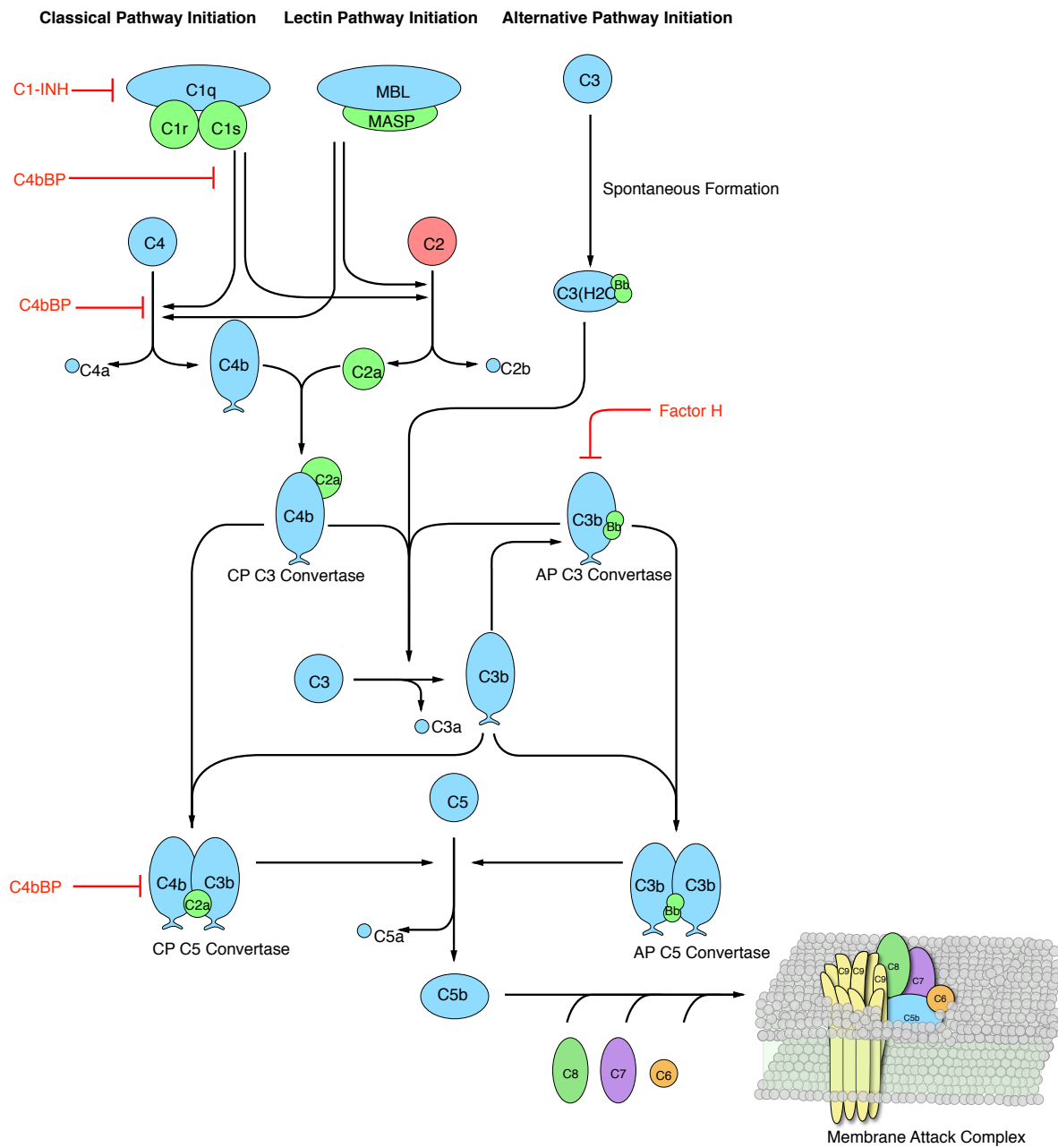


Fig. 1: Simplified schematic of the human complement system. The complement cascade is activated through any one, or more, of the three pathways: the classical, the lectin, and the alternate pathways. The classical pathway is activated by the binding of C1 complex through the C1q subunit to the IgG or IgM immune complex. This binding leads to conformational changes in the C1 complex that leads to the activation of C1r and C1s subunits. Activated C1-antibody complex cleaves C4 and C2 to form the classical C3 convertase. The lectin pathway is initiated by the binding mannose-binding lectins (MBL) and ficolins to carbohydrate moieties on the pathogen surfaces. This results in the formation mannose-binding lectin-associated serine proteases (MASPs). The MBL-MASP complex cleaves C4 and C2 to form the lectin C3 convertase. The alternative pathway is activated through a spontaneous tick-over mechanism by the hydrolysis of C3 to form fluid phase C3 convertase. The C3 convertases cleaves C3 into C3a, and C3b. C3b combines with C4b and C2a to form classical C5 convertase ($C_4bC_3aC_3b$). The C3b binds with Factor B to form the alternate C5 convertase ($C_3bB_bC_3b$).²⁷ The C5 convertases cleave C5 into C5a, and C5b that undergoes a series of reactions to form the membrane attack complex (MAC).

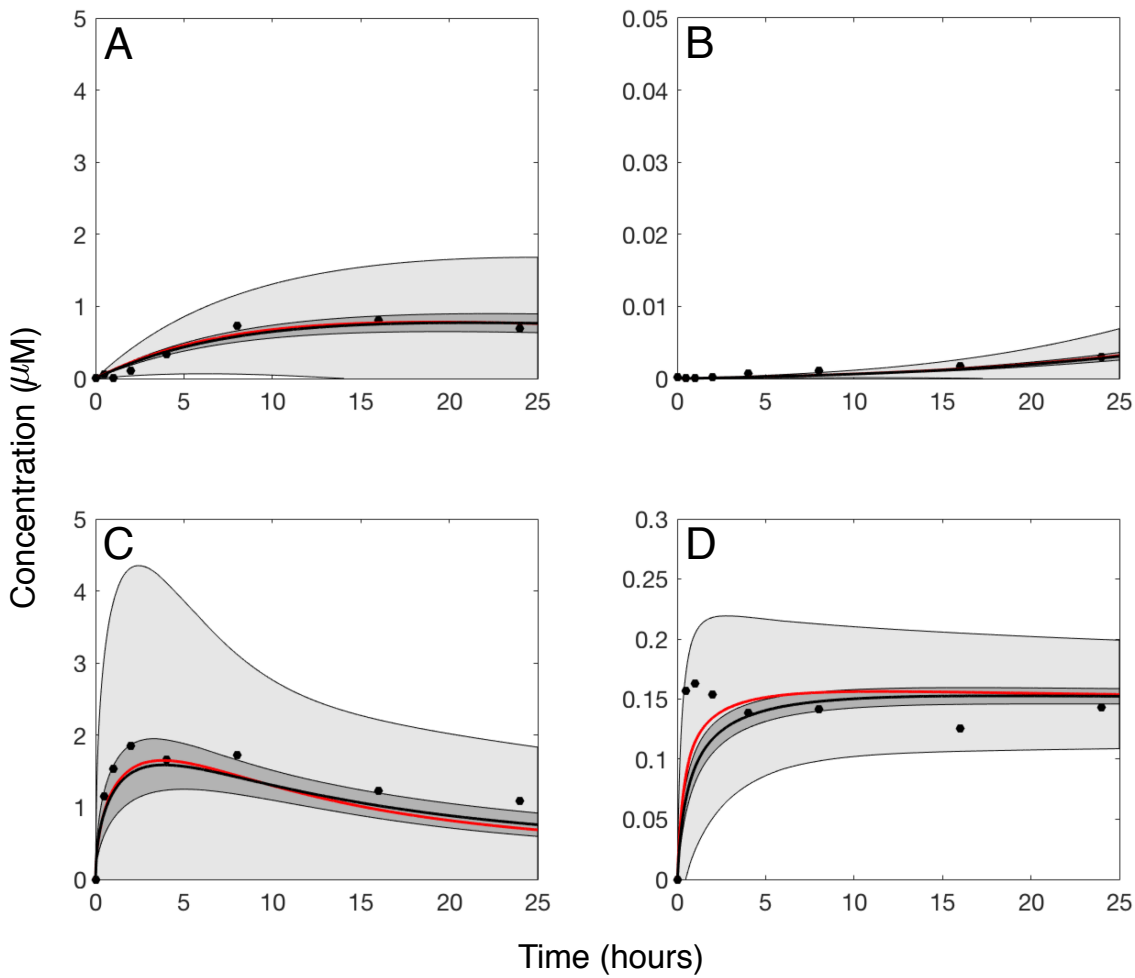


Fig. 2: Reduced order complement model training simulations. Reduced order complement model parameters were estimated using Dynamic Optimization with Particle Swarms (DOPS). The model was trained against experimental data from Shaw and co-workers (20) in the presence and absence of zymosan. The model was trained using C3a and C5a data generated from the alternative pathway (**A–B**) and lectin initiated pathway with 1g zymosan (**C–D**). The solid red line shows the simulation with the best-fit parameter, the solid black lines show the simulated mean value of C3a or C5a for 50 independent particles. The dark shaded region denotes 99 % confidence interval of the simulated mean concentrations of C3a or C5a , while the light shaded region is the 99 % confidence interval of the best prediction. All initial concentrations of complement proteins are at human serum levels unless otherwise noted.

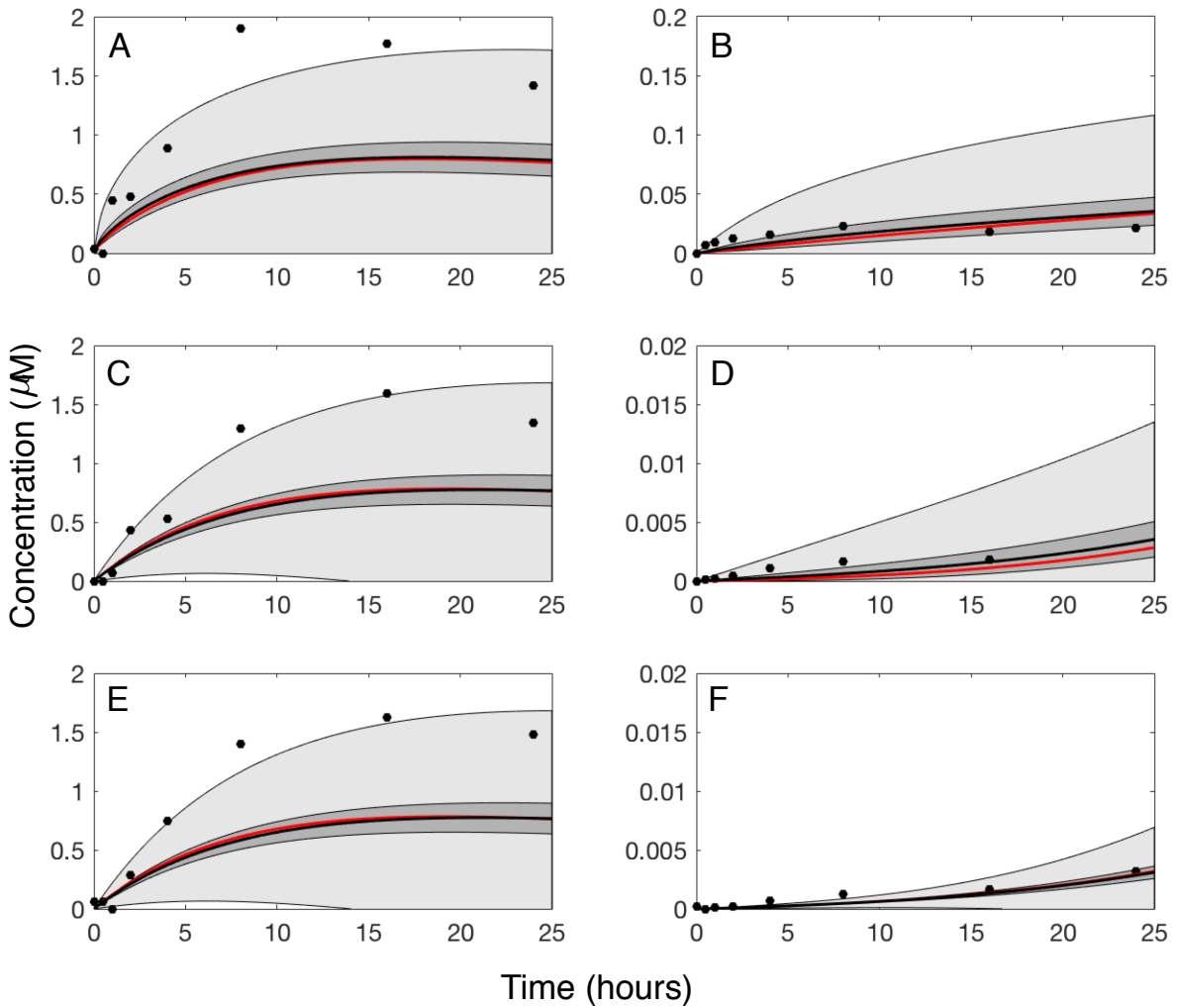


Fig. 3: Reduced order complement model predictions vs experimental data for C3a and C5a generated in the lectin pathway. The reduced order coagulation model parameter estimates were tested against data not used during model training. Simulations of C3a and C5a generated in the lectin pathway using different levels of zymosan (0.1, 0.01, and 0.001 grams of zymosan) were compared with the corresponding experimental data (A–F). The solid red line shows the simulation with the best-fit parameter, the solid black lines show the simulated mean value of C3a or C5a for 50 independent particles. The shaded region denotes 99 % confidence interval of the simulated mean concentrations of C3a or C5a, while the light shaded region is the 99 % confidence interval of the best prediction. All initial concentrations of complement proteins are at human serum levels unless otherwise noted.

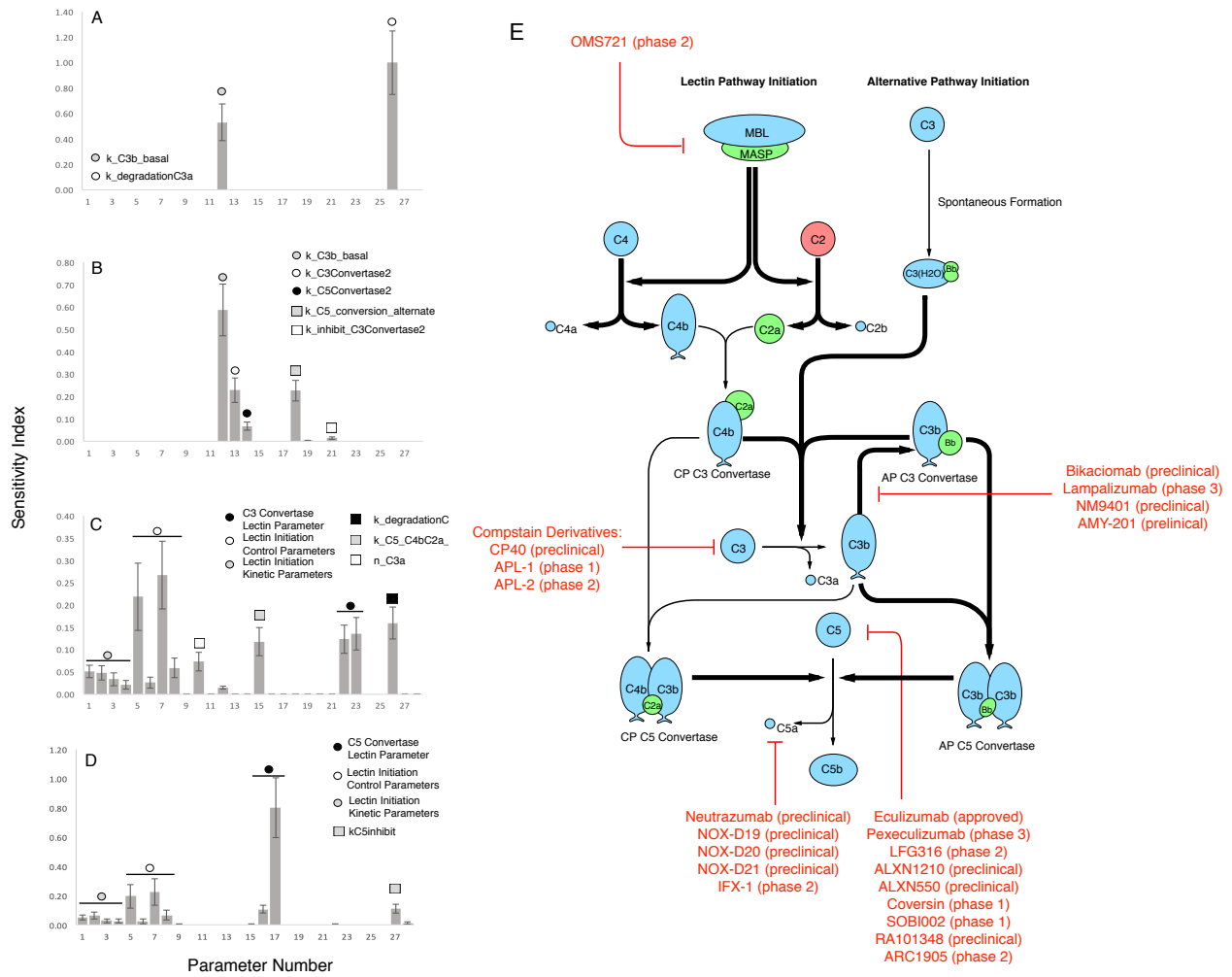
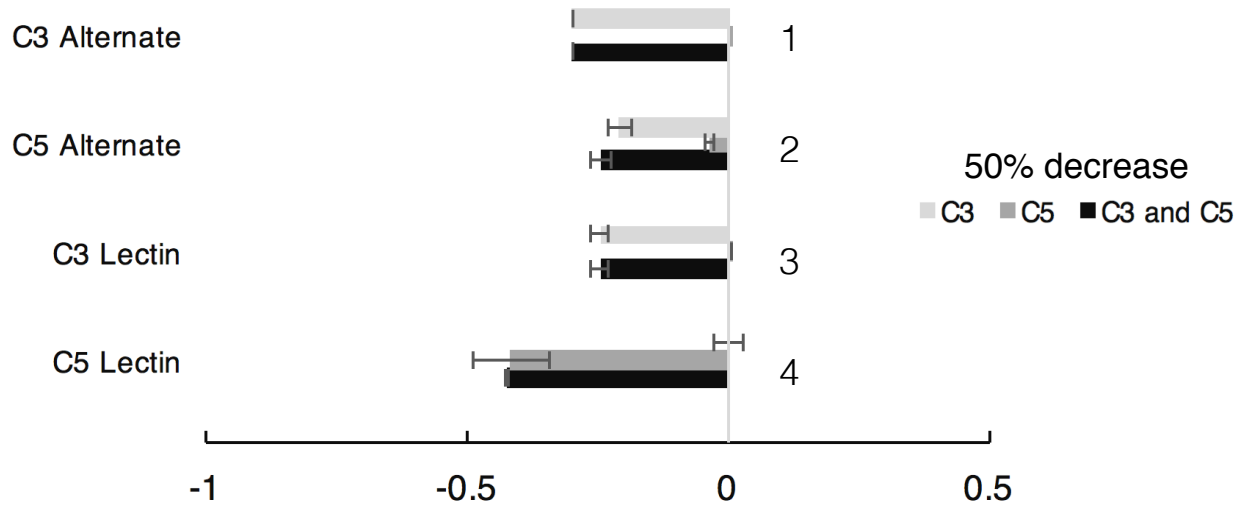


Fig. 4: Sobol's sensitivity analysis of the reduced order complement model with respect to the modeling parameters. Sensitivity analysis was conducted on the four cases we used to train our model: (A) C3a at 0g zymosan, (B) C5a 0g zymosan, (C) C3a 1g zymosan, and (D) C5a 1g zymosan. The bars denote total sensitivity index which includes local contribution of each parameter and global sensitivity of significant pairwise interactions. The error bars are the 95 percent confidence interval. Pathways controlled by the sensitivity parameters (E): Bold black lines indicates the pathway is governed by one or more sensitive parameters and the red lines shows some of the current therapeutics targets. Red indicates current complement therapeutics.

A



B

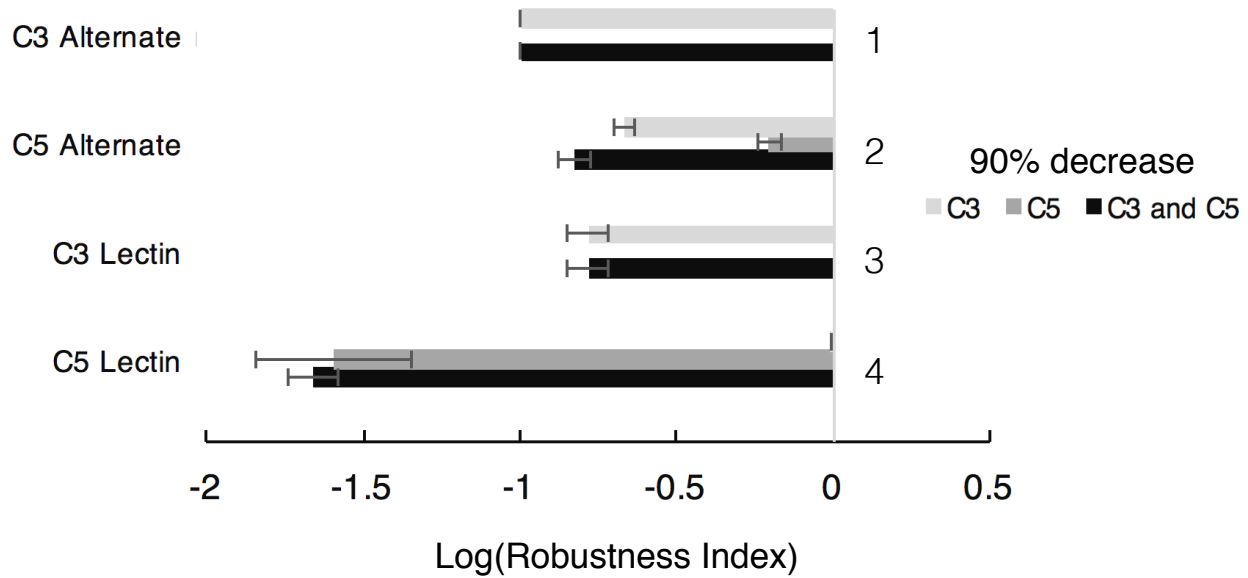


Fig. 5: Robustness analysis of the reduced order complement model with respect to the C3 and C5 initial concentrations using 50 parameter sets. Robustness analysis was conducted on the four cases we used to train our model, C3a alternate (0 zymosan), C5a alternate (0 zymosan), C3a lectin (1 g zymosan), and C5a lectin (1 g zymosan), by reducing the initial concentration of C3 and/or C5 by (A) 50 % and (B) 90 %. The bars denote robustness index which a measure of system changes from the perturbation of initial concentration that defined by the ratio of the area under the concentration curve of perturbed case and that of the unperturbed case. The error bars represent one standard deviation. At unity, the perturbed initial concentration has no impact on the measured output, and a robustness index lesser than or greater than one indicates a negative or positive relation between the perturbed initial concentration and the measured output respectively.

571 **Supplemental materials.**

572 **Model equations.** The reduced-order complement model consisted of 18 ordinary dif-
 573 ferential equations, 12 rate equations, and two control equations:

$$\frac{dx_1}{dt} = -r_1 f_1 \quad (\text{S1})$$

$$\frac{dx_2}{dt} = -r_2 f_2 \quad (\text{S2})$$

$$\frac{dx_3}{dt} = r_1 f_1 \quad (\text{S3})$$

$$\frac{dx_4}{dt} = r_1 f_1 - r_6 \quad (\text{S4})$$

$$\frac{dx_5}{dt} = r_2 f_2 - r_6 \quad (\text{S5})$$

$$\frac{dx_6}{dt} = r_2 f_2 \quad (\text{S6})$$

$$\frac{dx_7}{dt} = r_3 - r_4 - r_5 \quad (\text{S7})$$

$$\frac{dx_8}{dt} = r_3 + r_4 + r_5 - k_{deg,c3a} * C3a \quad (\text{S8})$$

$$\frac{dx_9}{dt} = r_3 + r_4 + r_5 - r_7 \quad (\text{S9})$$

$$\frac{dx_{10}}{dt} = r_6 - r_{10} - r_8 \quad (\text{S10})$$

$$\frac{dx_{11}}{dt} = r_7 - r_{11} - r_9 \quad (\text{S11})$$

$$\frac{dx_{12}}{dt} = r_{10} - r_{14} \quad (\text{S12})$$

$$\frac{dx_{13}}{dt} = r_{10} \quad (\text{S13})$$

$$\frac{dx_{14}}{dt} = -r_{12} - r_{13} \quad (\text{S14})$$

$$\frac{dx_{15}}{dt} = r_{12} + r_{13} - k_{deg,c5a} \quad (\text{S15})$$

$$\frac{dx_{16}}{dt} = r_{12} + r_{13} \quad (\text{S16})$$

$$\frac{dx_{17}}{dt} = -r_8 - r_{14} \quad (\text{S17})$$

$$\frac{dx_{18}}{dt} = -r_9 \quad (\text{S18})$$

$$(\text{S19})$$

⁵⁷⁴ where the rate equations are given by:

$$r_1 = \frac{k_{i1}(C4)}{(K_{1s} + C4)} \quad (\text{S20})$$

$$r_2 = \frac{k_2(C2)}{(K_{2s} + C2)} \quad (\text{S21})$$

$$f_1 = \frac{Zymo^{\eta_1}}{(Zymo^{\eta_1} + \alpha_1^{\eta_1})} \quad (\text{S22})$$

$$f_2 = \frac{Zymo^{\eta_2}}{(Zymo^{\eta_2} + \alpha_2^{\eta_2})} \quad (\text{S23})$$

$$r_3 = k_3(C3) \quad (\text{S24})$$

$$r_4 = \frac{k_4(C3C_L)(C3^{\eta_3})}{(K_{4s}^{\eta_3} + C3^{\eta_3})} \quad (\text{S25})$$

$$r_5 = \frac{k_5(C3C_A)(C3)}{(K_{5s} + C3)} \quad (\text{S26})$$

$$r_6 = k_6(C4b)(C2a) \quad (\text{S27})$$

$$r_7 = k_7(C4b)(C2a) \quad (\text{S28})$$

$$r_8 = k_8(C3C_L)(C4b)(C4BP) \quad (\text{S29})$$

$$r_9 = k_9(C3C_A)(FactorH) \quad (\text{S30})$$

$$r_{10} = k_{10}(C3C_L)(C3b) \quad (\text{S31})$$

$$r_{11} = k_{11}(C3C_A)(C3b) \quad (\text{S32})$$

$$r_{12} = \frac{k_{12}(C5C_L)(C5^{\eta_4})}{(K_{12s}^{\eta_4} + C5^{\eta_4})} \quad (\text{S33})$$

$$r_{13} = \frac{k_{13}(C5C_A)(C5)}{(K_{13s} + C5)} \quad (\text{S34})$$

$$r_{14} = k_{14}(C5C_L)(C4BP) \quad (\text{S35})$$